Adsorption 7: 189–209, 2001

Surface Diffusion of Hydrocarbons in Activated Carbon: Comparison Between Constant Molar Flow, Differential Permeation and Differential Adsorption Bed Methods

D.D. DO* AND H.D. DO
Department of Chemical Engineering, University of Queensland, St. Lucia, Qld 4072, Australia

Received October 26, 2000; Revised June 18, 2001; Accepted June 18, 2001

Abstract. This paper presents the comparison of surface diffusivities of hydrocarbons in activated carbon. The surface diffusivities are obtained from the analysis of kinetic data collected using three different kinetics methods-the constant molar flow, the differential adsorption bed and the differential permeation methods. In general the values of surface diffusivity obtained by these methods agree with each other, and it is found that the surface diffusivity increases very fast with loading. Such a fast increase can not be accounted for by a thermodynamic Darken factor, and the surface heterogeneity only partially accounts for the fast rise of surface diffusivity versus loading. Surface diffusivities of methane, ethane, propane, n-butane, n-hexane, benzene and ethanol on activated carbon are reported in this paper.

Keywords: surface diffusion, activated carbon, differential adsorption bed, constant molar flow, differential permeation, surface diffusivity

1. Introduction

Diffusion of adsorbed species in porous solids, or more generally in an "adsorbed phase", is a topic of great importance in adsorption science. It is perhaps the least understood phenomena in mass transport in porous media. This is because of the complex interaction between the adsorbate molecule and the surface atoms, and the complexity of the surface. Furthermore, real surfaces are not simple as "ideal" surfaces because of the structural and energetic heterogeneity. One simple approach of dealing with the surface heterogeneity has been that where a distribution of energy of interaction between the solid and the adsorbate molecule is assumed, and then a surface diffusion model is built based on this distribution after an assumption is made about the diffusion path.

No matter what the mechanism of transport of the adsorbed molecules (whether it has diffusion or hydrodynamic origin or rate of entry and leaving micropore), its macroscopic flux can be described by the following Fickian type equation, written in terms of the gradient of the adsorbed concentration:

$$\mathrm{J}_\mu = -D_\mu \frac{\partial C_\mu}{\partial z} \tag{1}$$

where D_μ is the transport surface diffusivity, which is a function of temperature, surface concentration (and possibly gradient of surface concentration), the interaction between the adsorbate and the solid surface, and the structure of the solid surface. This equation is a simplistic way of expressing the diffusion flux of the adsorbed species. First, what is the functional form for the transport surface diffusivity? Secondly what physical significance does that diffusivity have? Thirdly and most importantly, not all adsorbed molecules have the same mobility in the porous media. For example, adsorbed molecules residing in small pores will have much lower mobility than those in larger pores. The consequence

*To whom correspondence should be addressed.

of this is that at very low loadings, where adsorbed molecules mostly reside in small pores (because of their stronger adsorption energy) and hence the transport of adsorbed molecules will be very low. On the other hand, when the loading is sufficiently high to the extent that larger pores now have significant quantity of adsorbed molecules, and as a result the transport of adsorbed molecules will be mostly contributed by those in larger pores, where it is expected that adsorbed molecules will exhibit greater mobility and the flux of adsorbed species is due to molecules in larger pores rather than due to *all* adsorbed molecules. We will present in this paper the experimental observations of surface diffusion obtained by a variety of techniques, and then offer some plausible explanation for the transport of adsorbed hydrocarbons in activated carbon. The techniques of differential adsorption bed, the constant molar flow and the differential permeation will be used in this work. The determination of transport diffusion coefficient for activated carbon must be done by isolating the pore diffusion flux from the total observed mass flux. This will be discussed later, but first we present briefly what has been done in the literature about the attempt to correlate the surface diffusivity.

For a given temperature, it is now known that the transport diffusivity in porous media usually increases with loading. This rate of increase varies greatly from system to system. Many work reported insignificant change in the transport diffusivity with loading, while others have reported significant increase, for example Do (1996) has reported fast increase of the transport diffusivity with loading for propane and butane in a commercial activated carbon. So what are the causes for these vastly different observations? Very often, the experimental details were not mentioned, and it is therefore difficult to evaluate the accuracy of data, and secondly the surface diffusion flux is usually obtained indirectly by subtracting the gaseous flux from the total measured flux. If the gaseous flux were incorrectly determined, the surface flux would be incorrectly determined. Although this can be overcome in some systems where the surface diffusion flux dominates the measured flux, problems still remain in systems where the contribution of the surface diffusion flux is low at low loadings and very high at high loadings. The gaseous contribution can be determined by using the non-adsorbing gas such as helium and then extract the structural parameters for Knudsen diffusion and viscous flow. Then by assuming the diffusion and flow paths for the adsorbate are the same as those for helium, one can theoretically determine the Knudsen diffusion flux and viscous flow flux for the adsorbate provided that adsorbed molecules do not reduce the area for diffusion and flow to any extent. This in principles should work for most systems where the flow paths between the adsorbate and helium are generally the same.

1.1. The Correlative Models

Before we present our investigation of surface diffusion of hydrocarbons on activated carbon, we would like to briefly present various correlative models available in the literature. Our emphasis is on surface diffusion in activated carbon, and we will particularly discuss their inability to describe well surface diffusion of hydrocarbons in activated carbon.

1.1.1. Darken-type Theories. One of the earliest models for describing surface diffusion is that of Darken, and it assumes the gradient of chemical potential being the true driving force for diffusion. The surface diffusivity of this model has the following form:

$$D_\mu = D_\mu^0 \frac{\partial \ln P}{\partial \ln C_\mu} \tag{2a}$$

The following equation was derived to relate the transport diffusivity in terms of the so-called corrected diffusivity D_μ^0 (which is taken by Darken and many later researchers as independent of loading) and the thermodynamic correction factor $\partial \ln P / \partial \ln C_\mu$, which is known to increase with loading for convex isotherms. For systems where the adsorbed concentration is related to the gaseous pressure according to a Langmuir equation, the transport surface diffusivity of Eq. (1) is reduced to the following well-known form:

$$D_\mu = D_\mu^0 \frac{1}{1 - C_\mu / C_{\mu s}} = D_\mu^0 \frac{1}{1 - \theta} \tag{2b}$$

Higashi et al. (1963) used a random hopping mechanism where adsorbed molecule in one site jumps to another vacant site. They derived the transport diffusivity, which is identical to the one obtained by Darken theory when Langmuir equilibrium is assumed between the two phases (Eq. 2(b)). It is interesting to note that the HIO theory did not assume any connection between the surface and the gaseous phase, and yet these two theories produce the same expression. The Darken relation or the HIO equation (2(b)) increases to

infinity when the surface loading has reached its maximum capacity. Recognising this problem, Yang et al. (1973) proposed a modification to the HIO theory by allowing a finite residence time between the molecule and the occupied site instead of zero residence time as assumed by Higashi et al. They derived the following equation for the transport surface diffusivity:

$$D_\mu = D_\mu^0 \frac{1}{1-\theta+a\theta} \tag{3}$$

Another approach, which also gives rise to expression similar to that of Darken, is that of Chen and Yang (1991) who used the transition state theory to derive the following concentration dependence for the transport surface diffusivity:

$$D_\mu = D_\mu^0 \frac{1-\theta+(\lambda/2)\theta(2-\theta)+H(1-\lambda)(1-\lambda)(\lambda/2)\theta^2}{[1-\theta+(\lambda/2)\theta]^2} \tag{4}$$

where $H(\,)$ is the Heaviside step function, and the parameter λ is a measure of the degree of blockage by another adsorbed molecule. This parameter is zero for pure surface diffusion where there is no effective blockage. For this case the transport surface diffusivity reduces to that of the HIO or Darken theory. Equation (4) for non-zero λ can yield many patterns for the surface diffusivity variation with loading. It increases with loading for small λ, with the largest increase corresponding to $\lambda = 0$, and decreases with loading for large λ (for example in small pore zeolite). What this means is that the Darken or the HIO model for surface diffusivity exhibits the fastest increase for the surface diffusivity. Our experimental results show a much faster increase than predicted by the Darken equation, making the Darken, HIO or the transition state model of Chen and Yang not suitable for the description of surface diffusion of hydrocarbons in activated carbon. Many attempts have modified these models by accounting for the surface heterogeneity, for example Seidel and Carl (1989), and Kapoor and Yang (1989). Kapoor and Yang assumed a parallel path model for surface diffusion, and then proposed the following equation for uniform energy of interaction between the adsorbate molecule and surface:

$$D_\mu = D_\mu^0 \left[1 + \frac{e^{2s\theta}-1}{e^s - e^{s(2\theta-1)}}\right] \qquad \text{and}$$

$$D_\mu = D_\mu^0 \left\{1 + \frac{2s}{e^s - e^{-s}}\left[\frac{e^{2s\theta}-1}{e^s - e^{s(2\theta-1)}}\right]\right\} \tag{5a}$$

for $a = 1/2$ and 1, respectively. Here the parameter "a" is the mean ratio between the activation energy for surface diffusion to the heat of adsorption, and the parameter s is the parameter characterizing the system heterogeneity. The fractional loading θ relates to the pressure according to the Unilan equation:

$$\theta = \frac{1}{2s}\ln\left(\frac{1+be^s \mathrm{P}}{1+be^{-s}\mathrm{P}}\right) \tag{5b}$$

where b is the mean adsorption affinity constant, $b = b_\infty \exp(E_\mathrm{m}/RT)$, with E_m being the mean adsorption energy. Even with this account of heterogeneity, the increase in the surface diffusivity can not be explained.

Instead of assuming a parallel path approach, Kapoor and Yang (1990) used the effective medium approach to obtain the overall surface diffusivity. Depending on the dimension of diffusion (one or two dimensional diffusion), they derived expression for the overall transport surface diffusivity versus loading. The EMA-1D (one dimension diffusion) exhibits a faster increase with loading than the EMA-2D does. The expressions for the surface diffusivity for the EMA-1D model are given below for $a = 1$ and $a = 1/2$, respectively:

$$D_\mu = D_\mu^0 \left\{\frac{e^s - e^{-s}}{2s\theta}\left[\frac{e^{2s\theta}-1}{e^s - e^{s(2\theta-1)}}\right]\right\} \tag{6a}$$

and

$$D_\mu = D_\mu^0 \left\{\frac{(e^{s/2} - e^{-s/2})\sqrt{y}}{\left[\tan^{-1}\left(\sqrt{ye^s}\right) - \tan^{-1}\left(\sqrt{ye^{-s}}\right)\right]}\right\}, \quad \text{where} \quad y = \frac{e^{2s\theta}-1}{e^s - e^{s(2\theta-1)}} \tag{6b}$$

The fractional loading is related to the pressure according to Eq. (5b). The expressions for the EMA-2D are given in Kapoor and Yang (1990) in implicit form. The increase of the surface diffusivity with loading of the EMA-2D behaves very much like the PPM model of Kapoor and Yang (1989). On the other hand, the increase of the EMA-1D is much greater. Nevertheless, the observed increase in the surface diffusivity has been even greater than the EMA-1D model.

1.1.2. Multilayer Theories. The approach discussed in point (1) treated surface adsorption as one single entity in the adsorbed phase. It is possible however that

when a site is already occupied with a molecule, another molecule hopping onto that site could also be adsorbed. This is the basis for a series of work by Okazaki and co-workers using a hopping model, and Chen and Yang using a transition state theory. Tamon et al. (1981) extended the random hopping model of HIO, and they obtained the following expression for the transport surface diffusivity:

$$D_\mu = D_\mu^0 \left\{ \frac{\theta_e}{\theta} \frac{e^{-aE/RT} - e^{-E/RT}}{(1 - e^{-E/RT})[1 - \theta_e(1 - \tau_1/\tau_0)]} \right\} \tag{7a}$$

where $\theta_e = \theta(1-x)$. The fractional loading is governed by the classical BET equation:

$$\theta = \frac{1}{(1-x)} \frac{C_{\text{BET}} x}{[1+(C_{\text{BET}}-1)x]}; \qquad x = \frac{P}{P_0} \tag{7b}$$

Chen and Yang (1993, 1998) used the transition state theory to derive the following expression for the transport surface diffusivity of an open surface:

$$D_\mu = D_\mu^0 \left\{ \frac{1 - x + x/\alpha}{1 - (1-x)\theta + \alpha(1-x)\theta^2/[1-(1-x)\theta]} \right\} \tag{8a}$$

where x is the relative pressure P/P_0, and the parameter α $(0<\alpha<1)$ is given by:

$$\alpha = \exp[-(E_1 - E_2)/RT] \tag{8b}$$

The loading θ is related to the pressure via the BET equation (7b). Here E_1 is the activation energy for surface diffusion of the first layer, and E_2 is that for higher layers. This model predicts that the surface diffusivity approaches zero when the surface concentration reaches a maximum. When this happens, they argued that the overall flow may be determined from liquid phase diffusion model. The switch over to liquid flow might occur well before the surface concentration reaches its maximum value, and hence the dominance of the liquid-like flow is important at high loadings, where one would expect the hydrodynamic behavior of the flow.

1.1.3. Hydrodynamic Model. Gilliland et al. (1958) proposed a model whereby the flow of adsorbed molecules is due to the viscous motion of the liquid film inside the porous medium. The first distinction between this hydrodynamic model and the diffusion-type models is that the hydrodynamics model yields zero permeability at zero loading, while all diffusion-type models give non-zero permeability at zero loading. The expression for the apparent surface diffusivity has the form:

$$D_\mu = \beta \frac{C_\mu^2}{P} \tag{9}$$

The apparent surface diffusivity in Eq. (9) increases and then decreases with loading, instead of what is observed experimentally, that is increase with loading.

Another hydrodynamic model was proposed by Petropoulos (1996) for mesoporous solids. This is an extension to the model of Flood et al. (1952). The extension of homogeneous hydrodynamics model to allow for medium heterogeneity was carried out by Kainourgiakis et al. (1996) using a network model, Kainourgiakis et al. (1998) using a network model and percolation theory, and Kikkinides et al. (1997) using an effective medium theory.

1.1.4. Statistical-Mechanical Approach. All models discussed so far do not contain explicit information on the properties of diffusing adsorbate and temperature. Statistical-mechanical approach by Popielawski and Baranowski (1965), Popielawski (1966), Hwang and Kammermeyer (1966), and Lee and O'Connell (1972, 1975, 1986) provide partially this answer, for example Hwang and Kammermeyer obtained the explicit dependence of the surface diffusion in terms of temperature, and molecular weight as shown below:

$$D_\mu = \frac{\beta T \sqrt{T}}{\sqrt{M}} e^{-E_1/RT} \tag{10}$$

Here we see the dependence of the surface diffusivity on the inverse of the square root of the molecular weight, but we must note that their analysis was restricted to zero loading condition, where linear partition between the two phases is valid.

1.1.5. Knudsen Diffusion in Potential Field. Surface diffusion can be treated in conjunction with Knudsen diffusion of gaseous molecules diffusing in the environment where there is a potential energy of interaction between the diffusing molecules and the surface atoms. This approach has been studied by Weaver and Metzner (1966), Roybal and Sandler (1972), Shindo

et al. (1983), and Nicholson and Petropoulos (1973, 1975, 1979, 1981a, 1981b, 1985). Shindo et al. (1983) derived the following equation for the total permeability:

$$B = \frac{K}{\sqrt{MT}}\left[\frac{1}{1+\beta\varepsilon/RT} + \alpha\left(e^{\varepsilon/RT-1}\right)\right] \quad (11)$$

We note again the dependence on the molecular weight. This equation for permeability includes the transport of the gas molecules as well as molecules subject to the force field. If the force field is zero, the permeability will be that for Knudsen flow. Thus the difference between non-zero potential field and zero potential field is that contributed by the surface diffusion. This surface permeability is:

$$B_\mu = \frac{K}{\sqrt{MT}}\left[-\frac{\beta\varepsilon/RT}{1+\beta\varepsilon/RT} + \alpha\left(e^{\varepsilon/RT}-1\right)\right] \quad (12)$$

As seen from this equation that if the parameter β is very large and α is very small the surface diffusivity can be negative, suggesting that the flow under the external field can be lower than that when it is absent (Nicholson and Petropoulos, 1981, 1985).

1.1.6. Structural Approach. The various approaches dealt with so far do not address the structure of the solid medium. Do (1996) proposed a model for activated carbon, and addressed the effect of structure on the transport surface diffusivity. This model is similar to the approach done by Barrer (1987) and Karger (1988). Details of this model can be found in Do. The surface diffusivity takes the following form for the case where the equilibria is described by the Toth equation:

$$D_\mu = \frac{1}{a + b(1-\theta^t)^{1/t+1}} \quad (13)$$

1.2. This Paper

This paper will address the overall results of surface diffusion obtained in our laboratories from the various methods. The next section will discuss briefly the experimental technique, and Section 3 will present an overall theory and concept about surface diffusion in activated carbon, from which the experimental results will be interpreted upon.

2. Experimental Methods

The two aspects of adsorption, equilibria and kinetics, are needed for the analysis of surface diffusion. The equilibrium measurements were done with the high accuracy volumetric apparatus. The apparatus was assembled with VCR components and high quality vacuum valves to ensure the reliability of data at low pressures, and the pressure measurements were done with high accuracy MKS Baratron transducers type 690. The kinetics measurements were done with three different techniques. One is the differential adsorption bed method (DAB), developed in 1985 (Mayfield and Do, 1985) and successfully applied by Do and co-workers (Hu and Do, 1993; Do and Wang, 1998a, 1998b; King and Do, 1999). The second technique is the constant molar flow method, developed by Do (1995) and successfully applied by Prasetyo and Do (1998, 1999). The third technique is the differential permeation method. Among the three kinetic measurements, the DAB and CMF methods involve the mass transfer into a particle while the differential permeation involves the mass transfer through the particle (see Fig. 1). In the DAB method the concentration is maintained constant in the bulk during the whole course of mass transfer and the amount adsorbed is directly measured (details will be described later). In the CMF method, the mass is introduced into the batch adsorber at a constant rate and the pressure in the bulk is measured. In the DP method, mass transfer is through the particle and the pressure of the downstream face of the particle is measured.

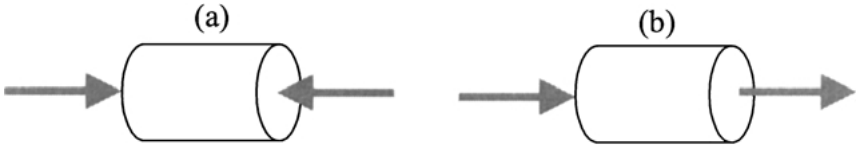

Figure 1. Mass transfer direction of DAB and CMF (a), and DP (b).

Usually the upstream face pressure is maintained constant with the use of a large source of adsorbate.

2.1. Volumetric Apparatus for Equilibria

A conventional high resolution volumetric adsorption rig with multiple sample cells was used to measure the pure component adsorption isotherms of hydrocarbons on a commercial Ajax activated carbon (type 976, Ajax Company, Australia). The rig consists of dosing and analysis sections and is made of VCR components suitable for very low pressure experiments. The system pressure is measured with high accuracy MKS Baratron pressure transducers. The general procedures of adsorption isotherm measurement are as follows: (1) the dosing section was filled (after evacuation and cleaning) with adsorbate. The number of moles of the adsorbate can be readily calculated from the knowledge of the dosing temperature, pressure and the volume of the section; (2) the isolation valve is slowly opened to allow N moles of adsorbate to enter the analysis section. After closing the valve, the N moles adsorbate dosed can be calculated from the knowledge of the initial and final pressures of the dosing section; (3) sufficient time is allowed for equilibrium to establish in the sample cell. Then the bulk pressure can be read from the pressure transducer and the amount adsorbed can be calculated from the knowledge of the N mole dosed and the number of moles left in the analysis section; (3) by repeating step (2)–(3) with different amounts of adsorbate dosed, the complete adsorption isotherm is obtained.

2.2. Differential Adsorption Bed (DAB)

A DAB rig was used to collect kinetic data, which consists of three main sections: gas mixing, collection and analysis. The principle of operation is to pass adsorbate gas over an adsorbent for a known duration of time, then to desorb, collect and analyse the quantity of adsorbed phase. Adsorbate gas flows at high rates to ensure adsorbent isothermality, remove stagnant layers and ensure a constant bulk concentration (the differential condition) making subsequent analysis easier. The mixing system consists of a bank of four MKS Instruments mass flow controllers (type 1259C). Feed gas from the mixing system then proceeds to the adsorption/collection section. Here, feed gas can either be vented, sent to gas chromatography (GC) for calibration or to the adsorber cell by appropriate valve manipulation. For a given time t, feed gas is passed through the sample cell containing adsorbent pellets then stopped by isolating the valve and venting the feed gas. Prior to and during adsorption, the adsorber cell is immersed in a water bath to maintain the adsorbent particles at a constant temperature. After adsorption has taken place and the cell isolated, a portable oven is placed around the cell which is then exposed to the previously evacuated sample bomb. A very slow purge of pure N_2 was required to assist desorption of adsorbate into the bomb. Once this has been achieved, the content of the bomb was sent to GC for analysis. The detailed experimental procedure is available in Do (1997). A typical uptake curve versus time obtained from this DAB technique is shown in Fig. 2.

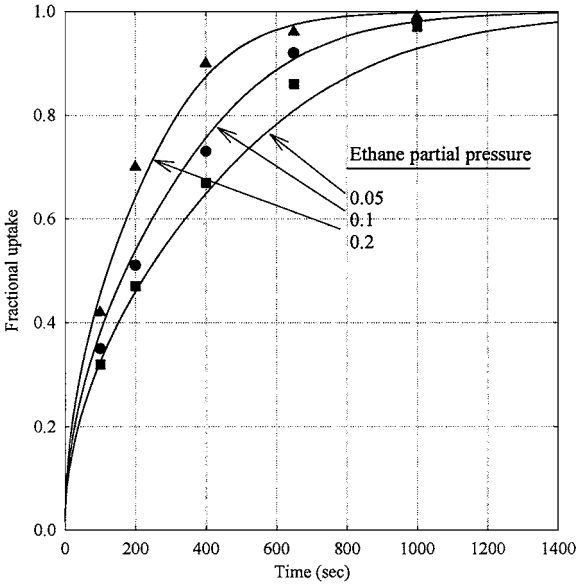

Figure 2. Typical fractional uptake versus time obtained by the DAB method. Ethane adsorption on slab activated carbon of length 4.4 mm at 283 K with ethane partial pressure (0.05, 0.1 and 0.2 atm) as parameter.

2.3. Constant Molar Flow Method (CMF)

The constant molar flow method was first conceived by Do (1995). This method is very simple in concept and operation. It involves basically a semi-batch adsorber, and a special leak valve which has the ability to supply a constant molar flow of pure adsorbate into the adsorber. The system pressure is monitored with a MKS Baratron transducer, and is logged into a personal

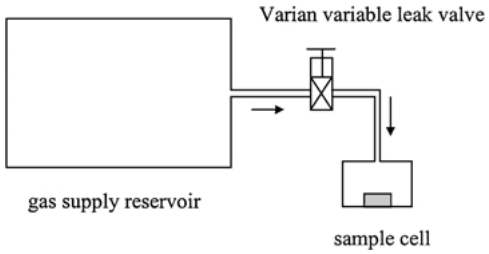

Figure 3. The concept of the constant molar flow method.

computer as a function of time, and such time trajectory will be used later for kinetics analysis. The system set-up is shown schematically in Fig. 3. It consists of two sections, the reservoir and adsorption sections separated by a vacuum variable leak valve (Varian model 951-5106). This valve controls very accurately low flows of adsorbate from the reservoir to the adsorption section. This is achievable with a moveable piston having an optically flat sapphire at the end and the valve body containing a metal gasket. The sapphire's movement is controlled through a threaded shaft-and-lever mechanism such that the gap between the sapphire and the metal gasket is very accurately controlled, resulting in an accurate low flow of adsorbate via Knudsen mechanism. The minimum leak rate of the valve is 1×10^{-10} torr-litre/sec and the vacuum range is from atmospheric pressure to below 10^{-11} torr, which is very suitable for the work in this study.

The range of flow rate is important in this study of kinetic parameter determination. If the flow is either too slow or too fast the pressure response will be linear over a practical time span. The linearity corresponding to very low flow is the result of quasi-equilibrium between the two phases and hence a linear pressure response. On the other hand the linearity corresponding to very large flow is due to the physical filling of the volume space in the adsorption cell. It is simple in experiment to obtain the range of flow rates for the purpose of kinetic parameter determination. More details can be found in Prasetyo (2000). The operation is briefly as follows. In each run, the sample was first degassed overnight at 150°C and at a pressure of about 10^{-5} torr. At $t = 0^+$, a constant molar flow of adsorbate from the reservoir was introduced into the adsorber, and the pressure was monitored and logged into a PC. The sample was then cleaned and ready for another run. The measurement was reproducible with a standard deviation of less than 2%. A typical pressure response for n-butane in activated carbon versus time is shown in

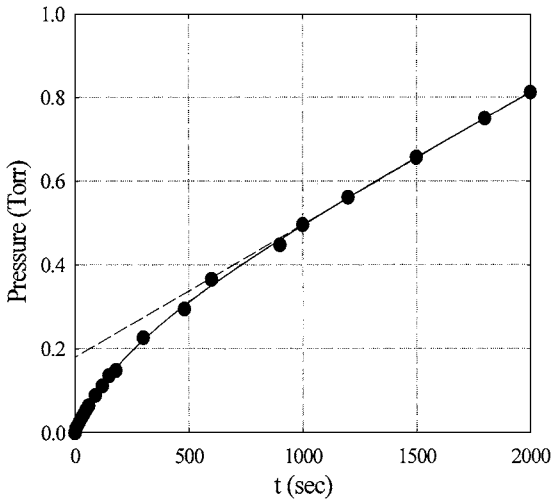

Figure 4. Typical pressure response versus time for the constant molar flow method for n-butane adsorption in activated carbon (Do, 2000).

Fig. 4. It has a pattern of an initial rise and then level off to reach a linear asymptote.

The slope and the intercept of this asymptote are directly related to equilibria and kinetics (see Do, 1995 for details). The general concern in all mass transfer measurement in adsorption is the interference of the heat effect. To extract a reliable mass transfer parameters, the heat effect must be eliminated. We have shown above that the DAB method can be successfully operated under isothermal conditions due to the very high flow of adsorbate, which removes the heat released from adsorption most effectively. In this constant molar flow method, the pure adsorbate is introduced slowly into the adsorber, and with this slow introduction the heat released from adsorption can be readily dissipated, giving an isothermal condition for mass transfer measurement. The following Fig. 5 shows the particle temperature as a function of time when we introduce a very strong adsorbing n-hexane into the semi-batch adsorber. Different molar flow rates were used in that measurement. With the typical molar flow of less than 1×10^{-9} mol/s, the temperature rise is about 1 degree. For other weaker adsorbing species, the temperature rise is much smaller. This can be regarded as an isothermal operation.

The effect of molar flow rate does not affect the pattern of the system pressure rise as a function of time (Fig. 6). Both the slope and the intercept of the linear asymptote are proportional to the molar flow rate, and this can be used to check the validity of the technique.

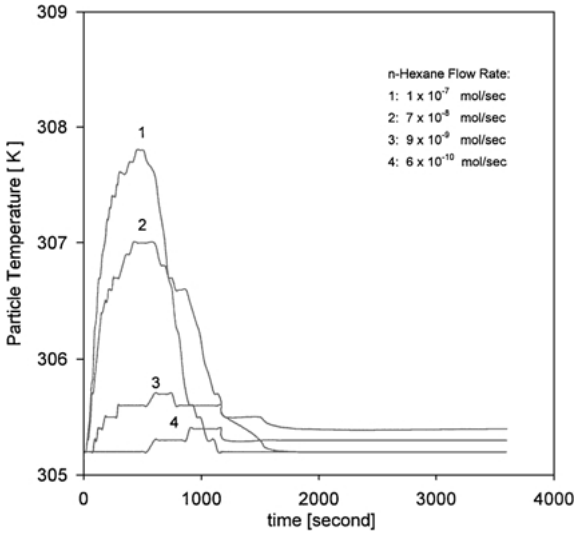

Figure 5. Particle temperature versus time for the method of constant molar flow of pure n-hexane.

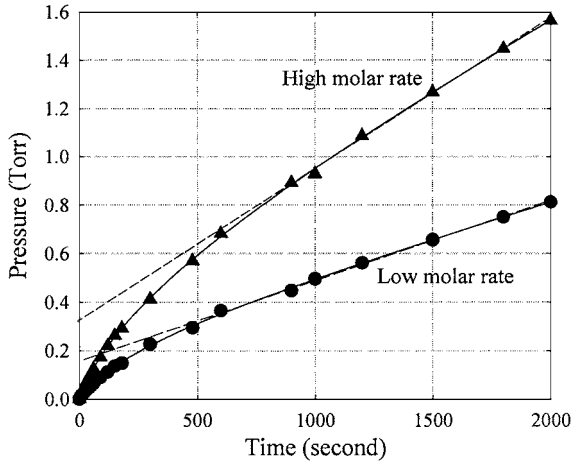

Figure 6. Effect of molar flow rate on the pressure response curve (Do et al., 2000).

The effect of particle size is typically shown in Fig. 7, where we see that the particle size does not affect the slope but it does affect the intercept of the linear asymptote. This is another test for checking the integrity of the technique as the slope contains information about the equilibria and hence it should be independent of the particle size. On the other hand, the intercept is related to kinetics and therefore it varies with particle size. According to the theory of Do (1995), this intercept is proportional to the square of the particle size, a typical property of all conduction and diffusion processes.

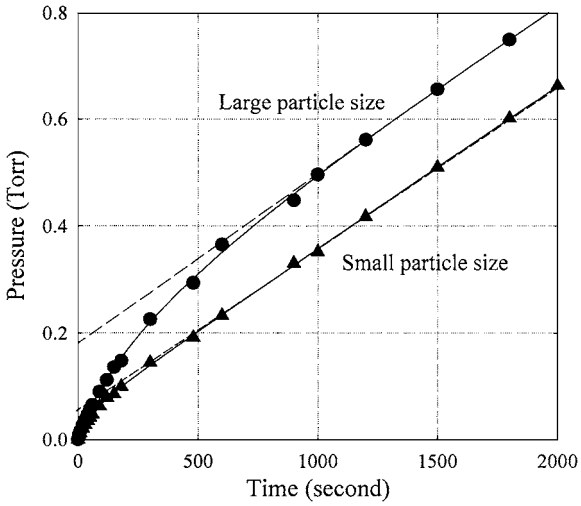

Figure 7. Effect of particle size on the pressure response curve.

The constant molar flow is a useful tool for the study of adsorption kinetics or pure gases and vapours. It is not restricted to runs at low pressure. Its versatility can be extended to pressure at any level. This is simply done by first equilibrating the system at some pressure, say P^*. Once this is achieved, a constant small flow of adsorbate is then introduced into the semi-batch adsorber, and the pressure is monitored versus time. Analysis of this pressure trajectory will yield kinetic parameter at that pressure P^* or at loading which is in equilibrium with P^*. Typical pressure responses as a function of time are shown in Fig. 8 for various levels of P^*.

From the analysis of these curves we can obtain the kinetic information, such as the surface diffusivity, as a function of loading.

2.4. *Differential Permeation*

The third technique that we used in the kinetic measurement is the differential permeation method. The experimental set-up is shown in Fig. 9. This ultrahigh vacuum (UHV) rig was constructed by using Cajon®; VCR®; fittings and ConFlat®; fittings. The system pressure is monitored by using the MKS Baratron®; pressure transducer type 690A and 698A. The apparatus consists of two compartments separated by the porous medium. The LHS reservoir is much larger than the RHS reservoir, such that the pressure of the LHS reservoir does not vary during the course of diffusion and adsorption.

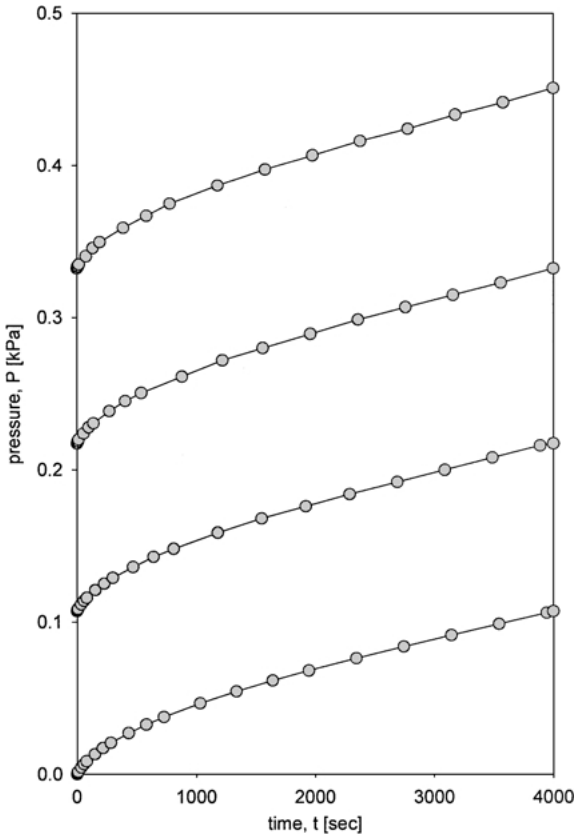

Figure 8. Pressure response versus time for various levels of P^*.

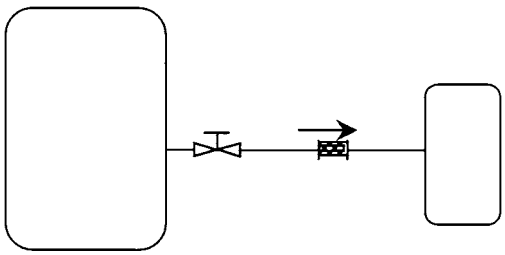

Figure 9. Schematic diagram of the permeation apparatus.

In each run, the sample was first degassed overnight at 150°C and at a pressure of at least 10^{-5} torr. After the porous particle has been cleaned, the upper compartment was filled with a small dose of gas or vapour, and at $t = 0^+$ the valve is opened to allow the gas or vapour diffusing through the porous medium. The pressure in the two compartments and the pressure difference are monitored and logged into a personal computer using a multi-channel data logger. The upper compartment pressure is essentially constant during

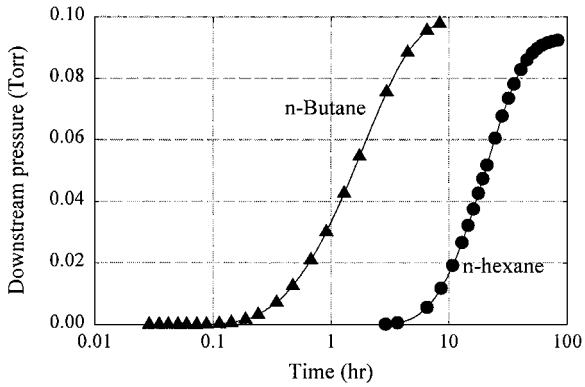

Figure 10. Downstream pressure response versus time for adsorbates of different affinity (n-hexane has higher affinity than propane).

the course of adsorption. The run is stopped when the downstream reservoir is equal to the upstream reservoir. The valve is then closed, isolating the upstream reservoir from the rest of the system. The pressure of the LHS compartment is then incrementally increased, and the valve is reopened allowing another run to take place. By repeating this procedure, we will obtain the flux and hence the permeability at various surface loadings. This concentration dependent permeability is then analysed for the separate contribution of the pore volume diffusion and the surface diffusion.

The typical response of the downstream reservoir is shown in Fig. 10. Here we show the responses for n-butane and strong adsorbing n-hexane. Because of its higher affinity, n-hexane will penetrate through the particle at a later time than that required for n-butane to break through. This pressure response curve has a typical sigmoidal shape, and how strong this sigmoidal is depends on the affinity of the adsorbate towards the solid as well as the kinetic properties of the adsorbate.

Figure 11 shows typical responses when the experimental runs are carried out at different initial loadings. For example, curve A is the response when the initial loading is 0 Torr, curve B is when the loading is 1.5 Torr, and so on. By analysing these curves, we can determine the kinetics parameters, especially the surface diffusivity, as a function of loading.

2.5. *Surface Diffusion Flux Calculation Procedure*

In all three methods used for kinetics measurement, the observed flux is the sum of pore diffusion, viscous flow and surface diffusion fluxes. The relative contribution of three processes depends on the operating conditions

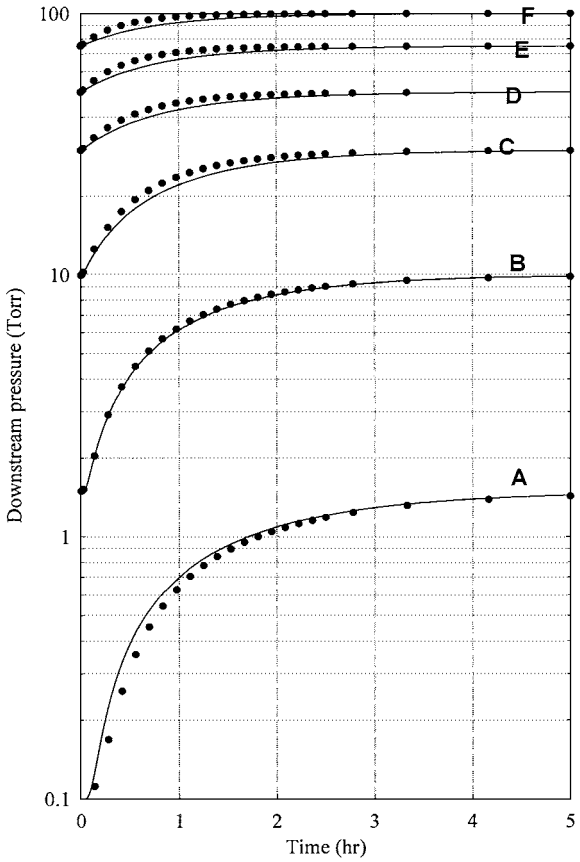

Figure 11. Plots of downstream pressure versus time for propane at 303 K for different initial loadings (Curve A: initial loading 0 Torr; curve B: initial loading 1.5 Torr; Curve C: initial loading 10 Torr; Curve D: initial loading 30 Torr; Curve E: initial loading 50 Torr and Curve F: initial loading 75 Torr).

as well as on the solid and adsorbate properties. Since pore diffusion and viscous flow are fairly well understood, we can isolate the flux contribution of these two processes from the total flux and thence the surface flux can be calculated. Using Eq. (1) then allows us to determine the transport diffusivity. In this section we will describe very briefly the procedure on how surface diffusivity is derived.

The general flux equation commonly used to describe the total flux contributed by the pore diffusion, viscous flow and surface diffusion is the one that assumes the three processes are additive, that is for a given pressure gradient, the flux is given by:

$$J = \left[\varepsilon\frac{D_{\rm p}}{RT} + \varepsilon\frac{B_0 P}{\mu RT} + (1-\varepsilon)D_\mu(C_\mu)\frac{dC_\mu}{dP}\right]\frac{\partial P}{\partial z} \tag{14}$$

The bracket term in the RHS of the above equation is called the total permeability. The first term in the bracket is the Knudsen diffusion permeability, the second viscous flow permeability and the last is the surface diffusion permeability. The pore diffusivity $D_{\rm p}$ is assumed to take the form, following Knudsen mechanism:

$$D_{\rm p} = \frac{4K_0}{3}\sqrt{\frac{8RT}{\pi M}} \tag{15}$$

where K_0 is called the Knudsen diffusion parameter. It is equal to $r/2$ for cylindrical pore where r is the pore radius, and $3r/8$ for slit pore where r is the half width (Nicholson and Petropoulos, 1985). For a general solid, the parameter K_0 will be treated as a fitting parameter to reflect all the solid characteristics, such as pore size, its distribution, pore shape and its distribution, pore orientation, pore surface roughness, etc. We will describe later how this can be determined. The parameter B_0 is the viscous flow parameter. It is equal to $r^2/8$ for cylindrical pore where r is the pore radius, and $r^2/3$ for slit pore where r is the pore half width. Like Knudsen diffusion parameter K_0, the viscous flow parameter B_0 will be determined experimentally.

To calculate the permeability contributed from surface diffusion, we need to isolate the pore Knudsen diffusion permeability and the viscous flow permeability. This is achieved by using helium as a non-adsorbing gas. Although helium is known to adsorb to some degree, but this only occurs in very fine pores (of dimension comparable to helium collision diameter) and at very low temperature (Kaneko et al., 1993). For the temperatures used in our experiment and fairly wide pore activated carbon, adsorption of helium is taken to be negligible (Ash et al., 1970). With helium used as the diffusing gas, the permeability is contributed by Knudsen diffusion and viscous flow only, and hence the flux for helium is simply:

$$J_{\rm He} = \left[\varepsilon\frac{D_{\rm p,He}}{RT} + \varepsilon\frac{B_0 P}{\mu_{\rm He} RT}\right]\frac{\partial P}{\partial z} \tag{16}$$

from which we can determine helium permeability as a function of pressure. Here $\mu_{\rm He}$ is the gaseous viscosity of helium. According to the above equation this relationship is linear. We carried out experiments of permeation with helium over a range of pressure at 303 K, and obtained the helium permeability as a function of pressure. The results are shown in Fig. 12, and it is clear from that figure that the relationship is indeed

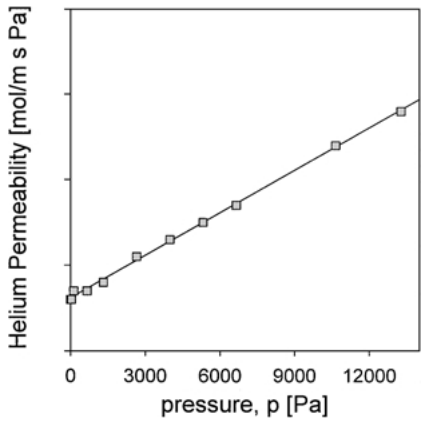

Figure 12. Helium permeability in Ajax activated carbon versus pressure at 303 K.

linear, conforming to the theory (Eq. (16)). From this straight line, we obtain the slope (S_{He}) and intercept ($B_{\mathrm{p,He}}$) for helium permeation. The intercept is the permeability contributed by Knudsen diffusion, while the viscous permeability is calculated from the slope as $B_{\mathrm{v,He}} = S_{\mathrm{He}} P$. Having obtained these, the Knudsen permeability and viscous flow permeability of any adsorbable gas or vapor are calculated from (to correct for adsorbate properties, molecular weight and viscosity):

$$\frac{B_{\mathrm{p}}}{B_{\mathrm{p,He}}} = \sqrt{\frac{M_{\mathrm{He}}}{M}}\sqrt{\frac{T_{\mathrm{He}}}{T}}; \qquad B_{\mathrm{v}} = \left(S_{\mathrm{He}}\frac{\mu_{\mathrm{He}}}{\mu}\frac{T_{\mathrm{He}}}{T}\right)P \tag{17}$$

Knowing these Knudsen diffusion and viscous flow permeabilities, the surface diffusion permeability is then calculated from Eq. (14).

3. A Mechanism for Surface Diffusion

To explain for the mobility of adsorbed molecules in activated carbon, we assume that such a mobility will have two components. One is due to the hydrodynamic nature of adsorbed molecules not adjacent to the solid surface, and the other is the diffusion component contributed by molecules adjacent to the surface. The diffusive component of the surface transport is assumed to take the form of Darken equation:

$$D_\mu = D_\mu^0 \frac{\partial \ln P}{\partial \ln C_{\mathrm{s}}} \tag{18}$$

where D_μ^0 is the corrected surface diffusivity, and C_{s} is the concentration of the first monolayer.

To derive the hydrodynamic component of the mobility of the adsorbed species, we assume that at local equilibrium the fugacity of the adsorbed phase (f_{A}) is related to the fugacity of the fluid phase as follows:

$$f_{\mathrm{A}} = f \exp\left(-\frac{\varphi}{kT}\right) \tag{19}$$

This fugacity of the adsorbed phase is much greater than the fluid phase fugacity, due to the potential energy of interaction between the adsorbate molecules and the surface atoms. This adsorbed phase fugacity is corresponding to a pressure in the adsorbed phase P_{A} (for example via equation of state), and the gradient of this pressure is responsible for the transport of the adsorbed phase. Assuming the transport in slit pores of activated carbon to follow that of Hagen Poiseuille flow, the average velocity is:

$$u_{\mathrm{A}} = -\frac{r^2}{3\mu_{\mathrm{A}}}\frac{\partial P_{\mathrm{A}}}{\partial z} \tag{20}$$

where μ_{A} is the viscosity of the adsorbed phase, and r is the pore physical half width. The mass flux $J_{\mathrm{A}} = \rho_{\mathrm{A}} u_{\mathrm{A}}$, where ρ_{A} is the molar density of the adsorbed phase, is given by:

$$J_{\mathrm{A}} = -\frac{r^2}{3\mu_{\mathrm{A}}}\rho_{\mathrm{A}}\frac{\partial P_{\mathrm{A}}^{\mathrm{DEF}}}{\partial z} = -D_\mu \frac{\partial \rho_{\mathrm{A}}}{\partial z} \tag{21}$$

Therefore, the surface diffusivity contributed by the hydrodynamic mechanism is:

$$D_\mu = \frac{r^2 \rho_{\mathrm{A}}}{3\mu_{\mathrm{A}}}\frac{\partial P_{\mathrm{A}}}{\partial \rho_{\mathrm{A}}} \tag{22}$$

If the adsorbed phase is treated as liquid, the RHS of the above equation can be evaluated using equation of state, such as the Peng-Robinson equation. Taking propane at 303 K, a pore of half width of 1 nm, and the fraction of pores having 1 nm is about 10%, Eq. (18) is calculated as 3×10^{-8} m^2/s. The viscosity of the adsorbed phase is taken as that of liquid phase at normal pressure. As will be seen later the surface diffusivity for propane at zero loading is 1.2×10^{-9} m^2/s, which is about 25 times smaller than that calculated using the hydrodynamic model. This suggests that at zero loading, the mechanism for adsorbed molecule mobility is diffusive in nature. At higher loadings, experimental value

for the surface diffusivity is in the range of $2. \times 10^{-9}$ to 5×10^{-8} m^2/s, into which the value calculated using the hydrodynamic model falls. This suggests that the mobility of adsorbed molecules will have two components: diffusive and hydrodynamic as follows:

$$D_\mu = \alpha \frac{r^2 \rho_A}{3\mu_L} \frac{dP}{d\rho_A} + \beta D_\mu^0 \frac{\partial \ln P}{\partial \ln C_s} \tag{23}$$

Following the statistical-mechanical treatment of Hwang and Kammermeyer, the corrected surface diffusivity D_μ^0 is inversely proportional to the molecular weight and its temperature dependence follows the Arrhenius law. The activation energy of the diffusive component is known to be a fraction of the heat of adsorption (Kapoor et al., 1989), while the temperature dependence of the hydrodynamic component will depend on the variation of the adsorbed viscosity.

The above equation describes the surface diffusivity if the transport of adsorbed species is governed by the combined mode of diffusion and viscous flow in micropores. When the molecular size is very much comparable to the pore dimension, the transport of molecules in and out of the micropores will be more dominating. If we assume the rate of entry and leaving the micropores to follow the Langmuir kinetics, then the apparent surface diffusivity due to this mechanism is (Appendix 1):

$$D_\mu = (k_a P + k_d) L_\mu / 2 \tag{24}$$

This component of surface diffusivity is greater with higher pressure (i.e. higher loading). At relative low loadings (i.e. low pressure) the temperature dependence also follows the Arrhenius law with the activation energy being the heat of adsorption because the rate constant for desorption is activated with the activation energy being the heat of adsorption. This means that if the observed activation energy for surface diffusion is approaching the heat of adsorption, the mobility of adsorbed molecules is then controlled by the entry into the micropore and evaporation from it.

4. Results

4.1. Adsorption Equilibria

Adsorption equilibria are obtained from high accuracy volumetric rig for methane, ethane, propane, n-butane, n-hexane, benzene and ethanol. Isotherms obtained for each adsorbate at at least three temperatures are shown in the following Fig. 13. The Henry constants obtained as the slope of the initial linear part of the isotherms are shown in Fig. 14, and also in Table 1. The heat of adsorption obtained from the change of the Henry constant with temperature is also shown in Table 1.

$$K = K_\infty \exp\left(\frac{Q}{RT}\right) \tag{25}$$

The heat of adsorptions are comparable to those obtained by Do and Do (1997) using the equilibria model of isosteric heat as a function of loading. Among the adsorbates studied here, n-hexane is the strongest adsorbing species, while ethanol has the highest heat of adsorption. This points to the fact that the adsorption mechanism of ethanol is not the same as that of the other hydrocarbons. This difference is in the extra electrostatic interaction between polar ethanol molecules with the functional groups on the carbon surfaces.

The adsorption isotherms are described very well with the Toth equation

$$C_\mu = C_{\mu s} \frac{bP}{[1 + (bP)^t]^{1/t}} \tag{26}$$

The parameters of these equations are optimally derived from the fitting of these equations against the experimental data, and these are listed in Table 2.

4.2. Surface Diffusivity at Zero Loading

We have discussed the equilibria of various hydrocarbons on activated carbon. Now we turn to the discussion of the surface diffusivity extracted from the analysis the kinetics data. Before discussing the surface diffusivity behaviour with respect to loading, we consider first the surface diffusivity at zero loading. The surface diffusivities obtained at zero loadings for the three kinetics methods are tabulated in Table 3, and typically shown in Fig. 15 versus $1/T$. From Table 3, we see that the values of the surface diffusivity obtained by these methods are very comparable to within about 50%. The difference in theses values is due to the different experimental procedure and also due to the fact that the contribution of the surface diffusion towards the total flux is between small to moderate (compared to pore volume diffusion flux and viscous flux) at zero loading, making the derivation of the surface diffusivity at zero loading from the total flux subject to some errors.

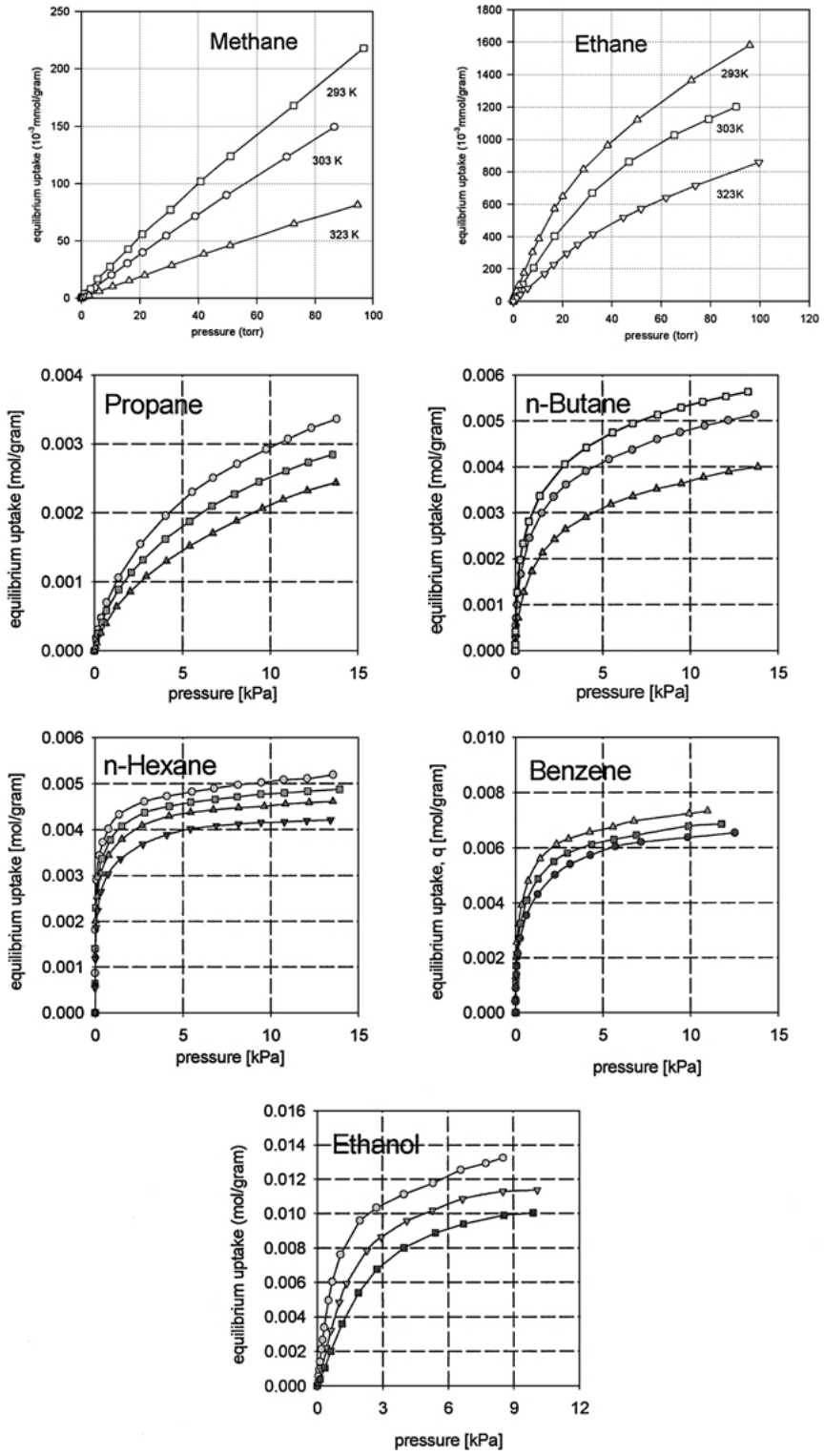

Figure 13. Adsorption isotherms of propane (303, 313, 323 K), n-butane (293, 303, 313 K), n-hexane (303, 313, 323, 333 K), benzene (313, 323, 333 K) and ethanol (303, 313, 323 K).

Table 1. Henry constant, heat of adsorption, surface diffusivity and its activation energy.

Species	T (K)	K	K_P (mol/g/Torr)	Q (J/mol)	Q (Do & Do, 1997)	D_μ (m^2/s)	E_μ (J/mol)
Methane	293	44	2.2×10^{-6}	24,700		1.3×10^{-8}	11,700
	303	39	1.88×10^{-6}			1.52×10^{-8}	
	323	20	9.08×10^{-7}			2.02×10^{-8}	
Ethane	293	772	3.86×10^{-5}	26,000	26,000	3.5×10^{-9}	13,400
	303	524	2.54×10^{-5}			4.21×10^{-9}	
	323	285	1.29×10^{-5}			5.86×10^{-9}	
Propane	293	5,742	2.87×10^{-4}	35,100	34,580	0.86×10^{-9}	21,300
	303	3,269	1.58×10^{-4}			1.15×10^{-9}	
	323	1,490	6.76×10^{-5}			1.94×10^{-9}	
n-butane	293	10,760	5.38×10^{-4}	42,260	43,000	1.025×10^{-10}	28,100
	303	6,550	3.17×10^{-4}			1.5×10^{-10}	
	323	2,130	9.67×10^{-5}			3.0×10^{-10}	
n-hexane	303	940,000	4.55×10^{-2}	50,600		8.6×10^{-12}	40,200
	313	500,000	2.34×10^{-2}			1.4×10^{-11}	
	323	270,000	1.23×10^{-2}			2.3×10^{-11}	
Benzene	303	98,250	4.75×10^{-3}	52,700		5.3×10^{-12}	43,900
	313	47,450	2.22×10^{-3}			8.9×10^{-12}	
	323	26,890	1.22×10^{-3}			1.56×10^{-11}	
Ethanol	303	9,194	4.45×10^{-4}	55,200		1.84×10^{-12}	52,300
	313	4,583	2.15×10^{-4}			3.57×10^{-12}	
	323	2,367	1.07×10^{-4}			6.65×10^{-12}	

$K = K_P \rho_P RT/(1-\varepsilon_m)$, where K_P is the slope of the plot C_μ (mol/g) versus pressure.

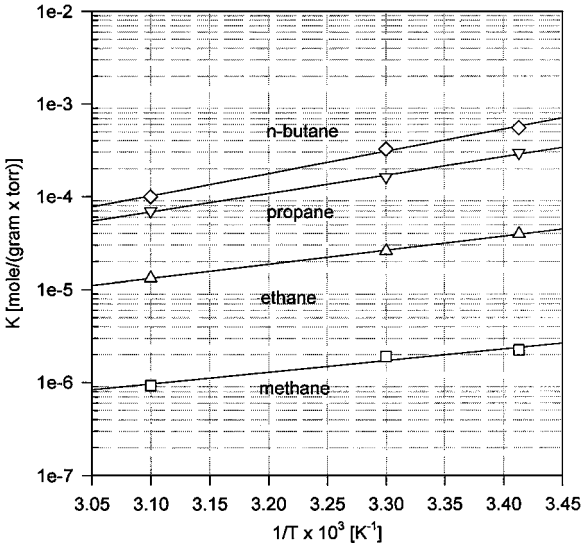

Figure 14. Plot of the Henry constants for methane, ethane, propane and n-butane versus $1/T$ (K).

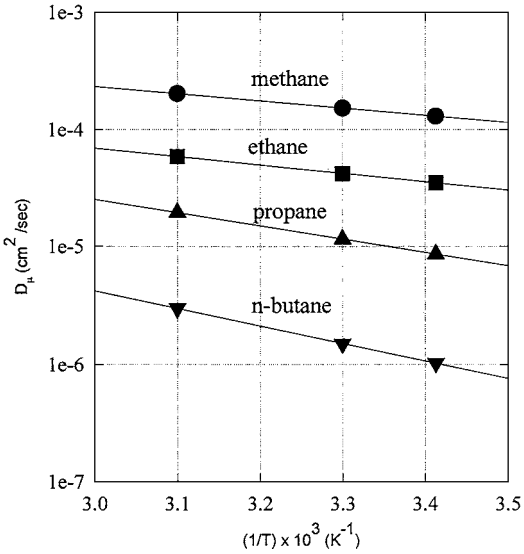

Figure 15. Plot of the surface diffusivity at zero loading versus $1/T$.

The plots of logarithm of the surface diffusivity versus $1/T$ (Fig. 15) show linearity over the narrow range of temperature. The activation energies obtained from the slope of those linear plots are shown in Table 4.

The activation energies for all these adsorbates are lower than the heat of adsorption, and these are compared graphically in Fig. 16(a). The ratio is shown in Fig. 16(b), and we note that this ratio increases from

Table 2. Optimal parameters of the Toth equation.

	303 K			313 K			323 K		
T	$C_{\mu s}$ (mol/cc)	b (1/Kpa)	t	$C_{\mu s}$ (mol/cc)	b (1/Kpa)	t	$C_{\mu s}$ (mol/cc)	b (1/Kpa)	t
Propane	0.0135	0.2519	0.368	0.0146	0.2044	0.340	0.0168	0.1038	0.340
n-butane	0.0111	10.09	0.294	0.0091	4.31	0.342	0.0078	2.29	0.383
n-hexane	.006776	1884.08	0.275	.006565	1283.62	0.276	.006113	502.41	0.304
Benzene	0.0112	141.86	0.313	0.0111	74.22	0.318	.010847	45.82	0.321
Ethanol	0.0160	0.9359	0.947	0.0130	0.4666	1.434	0.0115	0.3159	1.753

Table 3. Surface diffusivities derived from the three kinetics methods.

Species	D_μ (m^2/s) from CMF	D_μ (m^2/s) from DP	D_μ (m^2/s) from DAB
Ethane	4.21×10^{-9}	–	$3. \times 10^{-9}$
Propane	1.15×10^{-9}	2.8×10^{-10}	1.0×10^{-9}
n-butane	1.5×10^{-10}	2.0×10^{-10}	1.5×10^{-10}
n-hexane	1.4×10^{-11}	4.23×10^{-12}	–

Table 4. Activation energy for surface diffusion and heat of adsorption.

Species	E_μ (J/mol)	Q (J/mol)	E_μ/Q	ε_{fs}/k_B(K)
Methane	11,700	24,700	0.47	62
Ethane	13,400	26,000	0.52	77
Propane	21,300	35,100	0.61	81
n-butane	28,100	42,260	0.67	122
n-hexane	40,200	50,600	0.79	107

about 0.45 for methane to 0.8 for hexane. The approach of this ratio towards unity (that is the activation energy is approaching heat of adsorption) might indicate that when the molecular size is larger the mobility of adsorbed molecules is limited by its ability to enter to leave the micropores.

Since the interaction energy between the adsorbate and the solid is responsible for the adsorption and hence the mobility of the adsorbed molecules, we plot below in Fig. 17 the plots of activation energy and the heat of adsorption versus the interaction energy. Here we see that these energy parameters seem to correlate more linearly with each other, suggesting the adsorption mechanism as well as the diffusion mechanism of adsorbed species is probably associated with the dispersive force between the adsorbate molecules and the solid surfaces.

The question about the mobility of adsorbed species of whether it has origin from Knudsen mechanism is shown in Fig. 18, where the surface diffusivities are plotted versus the molecular weight and the hypothetical Knudsen diffusivities are also shown. The Knudsen diffusivities are calculated from:

$$D_K = \frac{2r}{3}\sqrt{\frac{8RT}{\pi M}} \tag{27}$$

where r is taken as the average pore size of micropores, which is taken to be 1 nm in this calculation. It is quite clear from this figure that Knudsen mechanism is not the mechanism for motion of adsorbed molecules as the calculated Knudsen diffusivities are at least two order of magnitude greater than the measured surface diffusivities.

To check whether the surface diffusivity would follow the inverse of the square root of molecular weight, we evaluate $D_\mu\sqrt{MW}$, and the results are shown in Table 5. We see that the surface diffusivity at zero loading decreases faster than the rate of inverse of the square root of molecular weight.

It must be remembered that the so-called surface diffusivity at zero loading should not be taken as that at absolute zero loading. This is due to two reasons. The first is that it is difficult to conduct experiments at ultra-low pressure to truly mimic the zero loading condition. Secondly, the mobility at "strictly" zero loading (that is the mobility of the first molecule adsorbed in the system) should be almost zero, because that molecule will adsorb onto the strongest site available in the system, which one would highly expect that the mobility is zero. Therefore, the so-called surface diffusivity at "zero-loading" should be taken at relative sense as possible.

From the results and observations obtained from the three kinetics methods of measurement, the surface

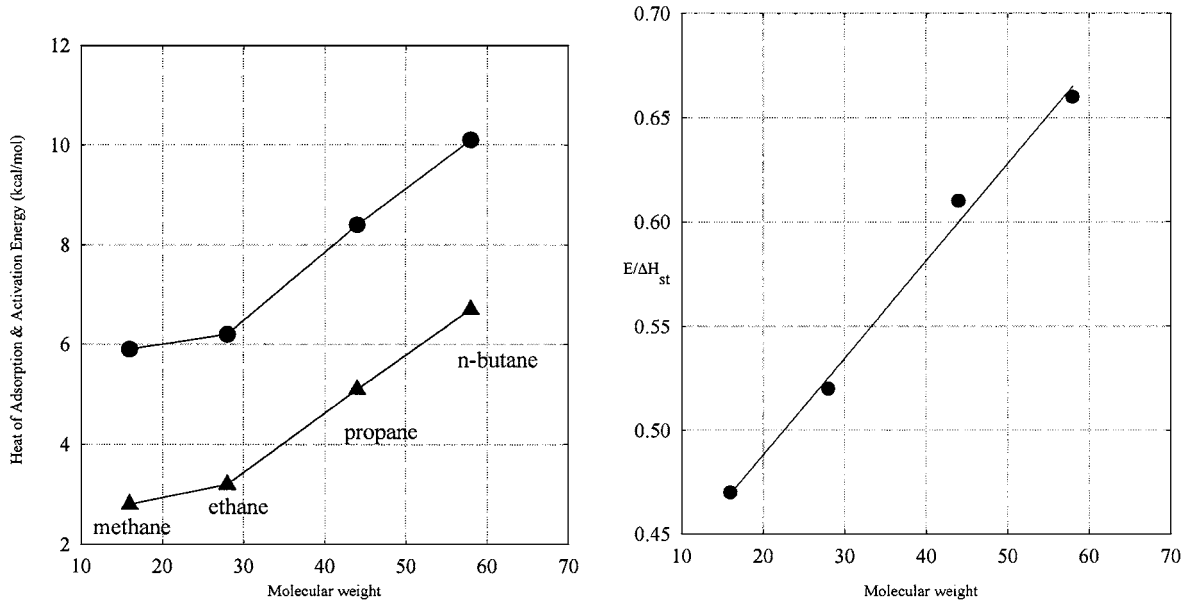

(a) (b)

Figure 16. (a) Activation energy and heat of adsorption versus molecular weight, (b) ratio of activation energy to heat of adsorption versus molecular weight.

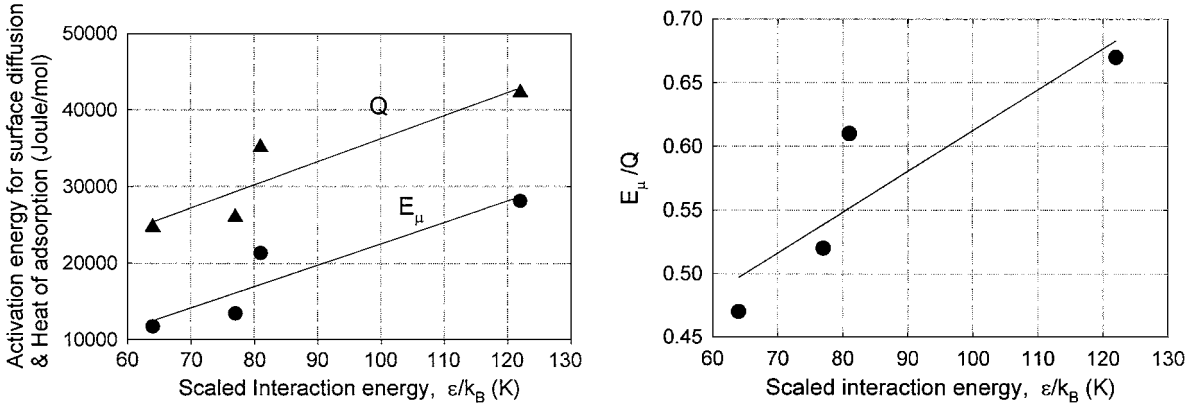

(a) (b)

Figure 17. (a) Plots of activation energy for surface diffusion and heat of adsorption versus scaled interaction energy, (b) plot of E_μ/Q versus scaled interaction energy.

diffusivity at zero loadings has the following characteristics.

1. *Apparent surface diffusivity increases with temperature for all adsorbates studied.* The functional dependence on temperature seems to follow the Arrhenius law, at least to be the case for the narrow range of temperature studied in our work
2. *Activation energy increases with molecular weight for the same class of adsorbate, and it is lower than the heat of adsorption*. The ratio of the activation energy to heat of adsorption is greater when the either the molecular weight increases or the molecular size increases. This ratio is approaching unity at large molecular size, suggesting that the activation energy for surface diffusion is close to the heat of adsorption. This indicates that the processes of entering and exiting the micropores are controlling. This makes sense because for any much larger molecules, the process will be one of sieving.

Table 5. Surface diffusivity at zero loading, and $D_\mu\sqrt{MW}$.

Species	T (K)	D_μ (m^2/s)	$D_\mu\sqrt{MW}$	E_μ (J/mol)
Methane	293	1.3×10^{-8}	5.2×10^{-8}	11,700
	303	1.52×10^{-8}	6.08×10^{-8}	
	323	2.02×10^{-8}	8.08×10^{-8}	
Ethane	293	3.5×10^{-9}	19.2×10^{-9}	13,400
	303	4.21×10^{-9}	23.1×10^{-9}	
	323	5.86×10^{-9}	32.1×10^{-9}	
Propane	293	0.86×10^{-9}	5.7×10^{-9}	21,300
	303	1.15×10^{-9}	7.63×10^{-9}	
	323	1.94×10^{-9}	12.9×10^{-9}	
n-butane	293	1.025×10^{-10}	6.8×10^{-10}	28,100
	303	1.5×10^{-10}	9.95×10^{-10}	
	323	3.0×10^{-10}	19.9×10^{-10}	
n-hexane	303	8.6×10^{-12}	79.8×10^{-12}	40,200
	313	1.4×10^{-11}	12.9×10^{-11}	
	323	2.3×10^{-11}	21.3×10^{-11}	

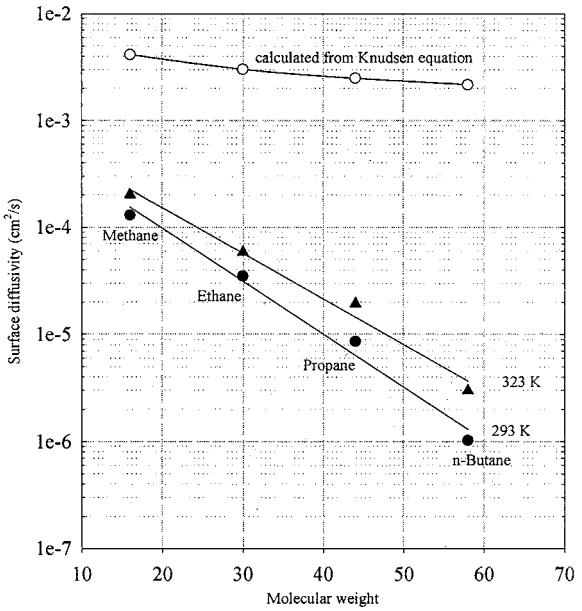

Figure 18. Plots of surface diffusivities and hypothetical Knudsen diffusivities versus molecular weight.

3. *Apparent surface diffusivity is generally small at zero loading*. It can be subject to some error. This is akin to the determination of the Henry constant in equilibria study.
4. *The contribution of surface diffusion at zero loading towards the total flux* is modest for low molecular weight hydrocarbons and is very low for high molecular weight species. But its contribution at higher loadings is much greater. This will be discussed in the next section on concentration dependence.
5. *Apparent surface diffusivity decreases very rapidly with molecular weight*, much stronger than $1/\sqrt{MW}$ as suggested by some surface diffusion theory, such as Hwang and Kammermeyer (1966).
6. *Apparent surface diffusivity is much lower than the calculated Knudsen diffusivity*, indicating that the process of surface diffusion does not follow Knudsen mechanism.

4.3. Surface Diffusivity at Higher Loadings

The observed surface diffusivities at higher loadings obtained by the constant molar flow method and differential permeation are shown in Fig. 19. The ranges of surface diffusivity obtained by both methods are comparable, and we list in Table 6 those ranges.

Table 6 shows that the surface diffusivity increases by about 2 to 3 orders of magnitude, indicating that the surface diffusion becomes dominant at higher loading. This illustrates that the surface diffusion should not be ignored in the modelling of kinetics in activated carbon.

Observation for surface diffusivity at higher loadings obtained by the three kinetics methods can be summarised below:

1. *Surface diffusivity increases very fast with loading*, usually at a rate much greater than what predicted by the Darken relation. This means that the thermodynamic correction factor in the Darken equation is not sufficient to explain for the increase. Solid heterogeneity only accounts partially for the strong concentration dependence of the surface diffusivity. This behaviour of very fast increase of D_μ with loading can only be described when the corrected surface diffusivity is assumed as a function of loading. This is feasible via the notion that the activation energy for surface diffusion is a function of loading (Do et al., 2000).
2. *The pattern of surface diffusivity has a rapid rise at a critical loading*, that is it takes the shape such that the surface diffusivity increases only modestly at low loadings but it then increases quite rapidly once a critical loading has been passed. This critical loading is higher for larger molecules, for example the critical loading for propane is 1500 mol/m^3 while that of n-hexane is 4000 mol/m^3. The rate of increase with loading is also greater with larger molecules, for example n-hexane and benzene compared to propane and n-butane.

Table 6. The range of surface diffusivities for propane, n-butane, n-hexane, benzene and ethanol at 303 K.

Species	Loading range (mol/m^3)	Range of D_μ (m^2/s) (CMF)	Range of D_μ (m^2/s) (DP)	Range of D_μ (m^2/s) (DAB)
Propane	$0 \rightarrow 3{,}500$	$10^{-9} \rightarrow 10^{-7}$	$10^{-9} \rightarrow 10^{-7}$	$10^{-10} \rightarrow 10^{-8}$
n-butane	$0 \rightarrow 5{,}000$	$10^{-10} \rightarrow 10^{-7}$	$10^{-10} \rightarrow 10^{-7}$	$10^{-10} \rightarrow 10^{-9}$
n-hexane	$0 \rightarrow 5{,}500$	$10^{-11} \rightarrow 10^{-7}$	$10^{-11} \rightarrow 10^{-7}$	–
Benzene	$0 \rightarrow 8{,}500$	$10^{-11} \rightarrow 10^{-8}$	$10^{-11} \rightarrow 10^{-7}$	–
Ethanol	$0 \rightarrow 14{,}000$	$10^{-12} \rightarrow 10^{-11}$	$10^{-11} \rightarrow 10^{-8}$	–

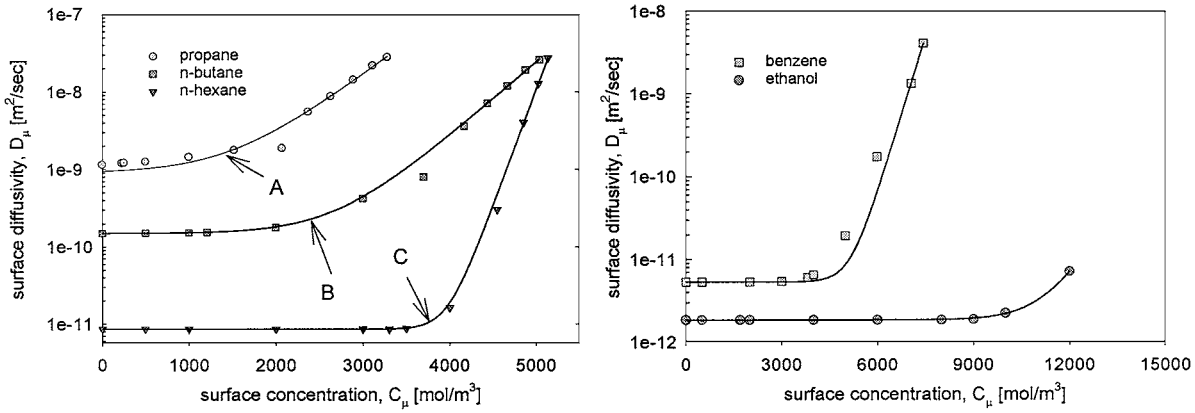

Figure 19. Apparent surface diffusivity of propane, n-butane, n-hexane, benzene and ethanol versus loading obtained by the CMF method and DP method.

3. *The polar component can affect the mobility of adsorbed molecules*. For example, we take propane and ethanol, having comparable molecular weights of 44 and 46, respectively. Propane has a surface diffusivity at zero loading of 1×10^{-9} m^2/s, while ethanol is 2×10^{-12} m^2/s (about 1000 times lower). The critical concentration of propane is 1500 mol/m^3, while that of ethanol is 9000 mol/m^3. This points to the strong interaction between polar ethanol with the functional groups on the surface. Since functional groups tend to be located near the edges of the graphitic layers (i.e. in the mouth of micropores), this again points to the importance of the processes of entering and exiting the micropores being the dominant process in the overall transport of adsorbed molecules. What this means is that the transport of adsorbed ethanol is governed by its ability to enter or exit the mouth of micropores, resulting in very low apparent surface diffusivity.
4. The concentration dependence of surface diffusivity versus loading is very much the same between the DP and the CMF methods. Since the DP method does not give accurate results at very low loadings, the behaviour at low loading for the DP method is not presented in the above figures. Nevertheless they both show very rapid increase with loading. The only significant difference between the two methods is ethanol, where the range of surface diffusivity is between 10^{-12} to 10^{-8} for the DP method, while this range is 10^{-12} to 10^{-11} for the CMF method. This is the subject for our future investigations.

Possible explanation for the critical concentration. Activated carbon is known to have distribution of micropores. For a given micropore, the adsorption affinity is greater and the mobility is lower for larger molecules compared to those of smaller molecules. To illustrate this, let us assume that micropores can be divided into four ranges of micropores, with each range having a capacity of 1 mmole/g.

At a loading of 1 mmole/g, the first range which is the smallest micropores is filled, and all species will have small contribution towards the diffusion flux because of the very tight pores, but the larger molecular weight

molecules will have the lowest mobility. At a loading of 2 mmole/g, when the first two ranges of micro-pores are now filled, lower molecular weight molecules in the second range now have greater mobility and will start to exert its contribution to the surface diffusion flux. This is the level where species such as propane will have its increase in the surface diffusivity. The second range is still too small for higher molecular species to exhibit any significant change in the surface diffusivity. At a loading of 3 mmol/g, when the third range now is filled with adsorbed molecules. The pore size is large enough for the higher molecular weight to exert its influence on the surface diffusion. This loading becomes the critical loading for the surface diffusivity of n-hexane. At any greater loading than 4 mmol/g, the diffusion of adsorbed species is now dominated by those residing inside the large micropores, i.e. the fourth range. In this range, the mobility of molecules is due those weakly bound to the surface of the pores and the flow is more towards the hydrodynamics nature. At this high level of loading, the transport of adsorbed molecules will have some hydrodynamic origin, and the apparent surface diffusivity is given by Eq. (22). This equation shows that higher molecular weight species can exhibit greater mobility, and this is reflected in Fig. 18, where n-hexane starts to have greater mobility than n-butane when the loading is greater than 5000 mol/m^3.

5. Conclusions

We have presented in this paper results of investigation into diffusion of adsorbed molecules in activated carbon. Three different methods for kinetics measurement were used in our investigation, and the surface diffusivities obtained from these are quite comparable. It is found that for hydrocarbons, the surface diffusivity has the following characteristics:

1. Apparent surface diffusivity increases with temperature for all adsorbates studied.
2. Activation energy increases with molecular weight for the same class of adsorbate, and it is lower than the heat of adsorption.
3. The activation energy is approaching heat of adsorptionunity at large molecular size, suggesting that the processes of entering and exiting the micropores are controlling.
4. Apparent surface diffusivity is generally small at zero loading.
5. The contribution of surface diffusion at zero loading towards the total flux is modest for low molecular weight hydrocarbons and is very low for high molecular weight species.
6. Apparent surface diffusivity decreases very rapidly with molecular weight, much stronger than $1/\sqrt{MW}$.
7. Apparent surface diffusivity is much lower than the calculated Knudsen diffusivity, indicating that the process of surface diffusion does not follow Knudsen mechanism.
8. Surface diffusivity increases very fast with loading, usually at a rate much greater than what predicted by the Darken relation.
9. The pattern of surface diffusivity has a rapid rise at a critical loading.
10. The polar component can affect the mobility of adsorbed molecules.

Appendix 1: Mass Transfer of Adsorbed Species via Micropore Entry and Evaporation

According to the model of Do (1996), one of the processes that is responsible for the transport of adsorbed molecules is the entry and evaporation from the micropore mouth of a graphitic unit. Let the length of the unit is L_μ. The rate of entry into one end of the unit is (assuming the rates follow Langmuir adsorption kinetics mechanism)

$$J_{\mu,1} = k_a P_1 (C_{\mu s} - C_\mu) - k_d C_\mu \tag{A1.1}$$

Similarly the rate of evaporation from the other end of the unit is:

$$J_{\mu,2} = k_d C_\mu - k_a P_2 (C_{\mu s} - C_\mu) \tag{A1.2}$$

where P_1 and P_2 are the adsorbate pressures at two ends of the unit. The rate constant for desorption k_d is assumed to follow:

$$k_d = k_{d,\infty} \exp\left(\frac{Q}{RT}\right) \tag{A1.3}$$

where Q is the heat of adsorption. In writing Eqs. (A1.1) and (A1.2), we have assumed that there is no mass transfer resistance inside the graphitic unit or it is negligible compared to the resistance of entry and leaving the unit. At quasi-steady, the net rate of entry (Eq. (A1.1)) is equal to the rate of leaving (Eq. (A1.2)).

Equating these two equations, we obtain an expression for the adsorbed concentration:

$$C_\mu = \frac{k_a C_{\mu s}(P_1 + P_2)}{(k_a P_1 + k_d) + (k_a P_2 + k_d)} \tag{A1.4}$$

Substituting this adsorbed concentration into either Eq. (A1.1) or (A1.2), we derive the following equation for the diffusion flux of adsorbed molecule across the graphitic unit:

$$J_\mu = \frac{k_a k_d C_{\mu s}}{2(k_a P + k_d)} \Delta P \tag{A1.5}$$

in which we have assumed that P_1 is very close to P_2. Expressing this flux in terms of the concentration gradient of adsorbed molecule across the graphitic unit, we have:

$$J_\mu = \frac{k_a k_d C_{\mu s}}{2(k_a P + k_d)} \Delta P = D_\mu \frac{\Delta C_\mu}{L_\mu} \tag{A1.6}$$

from which we can solve for the transport diffusivity:

$$D_\mu = \frac{k_a k_d L_\mu C_{\mu s}}{2(k_a P + k_d)\partial C_\mu / \partial P} = \frac{L_\mu k_d (1 + bP)}{2} \tag{A1.7}$$

In obtaining Eq. (A1.7), we have assumed the adsorption isotherm follows the Langmuir equation, which is consistent with the Langmuir kinetics as posed in Eqs. (A1.1) and (A1.2).

Notation

b	Adsorption affinity constant
B	Permeability
B_μ	Permeability contributed by surface diffusion
B_0	Viscous flow parameter
C_μ	Adsorbed concentration
$C_{\mu s}$	Maximum adsorbed concentration
D_p	Pore diffusivity
D_μ	Surface diffusivity
D_μ^0	Corrected diffusivity
k_a	Rate constant for adsorption
k_d	Rate constant for desorption
K	Henry constant
K_0	Knudsen diffusion parameter
L_μ	Length of one unit graphitic cell
M	Molecular weight
P	Pressure
P_0	Vapour pressure
Q	Heat of adsorption
r	Pore physical half width
R	Gas constant
t	Toth constant
T	Temperature
X	Reduced pressure $= P/P_0$
z	Distance

Greek Symbols

α, β	Constants
μ	Viscosity
φ	Potential energy
θ	Fractional loading

Acknowledgment

This project is supported by the Australian Research Council.

References

Ash, R., R.M. Barrer, and R.T. Lowson, "Diffusion of Helium Through a Microporous Carbon Membrane," *Surface Science*, **21**, 265–272 (1970).

Barrer, R.M., "Flow Into and Through Zeolite Beds and Compacts," *Langmuir*, **3**, 309–315 (1987).

Chen, Y.D. and R.T. Yang, "Concentration Dependence of Surface Diffusion and Zeolitic Diffusion," *AIChE Journal*, **37**, 1579–1582 (1991).

Chen, Y.D. and R.T. Yang, "Surface Diffusion of Multilayer Adsorbed Species," *AIChE Journal*, **39**, 599–606 (1993).

Chen, Y.D. and R.T. Yang, "Surface and Mesoporous Diffusion With Multilayer Adsorption," *Chem. Eng. Sci.*, **36**, 1525–1537 (1998).

Darken, L.S., "Diffusion, Mobility and Their Interrelation Through Free Energy in Binary Metallic Systems," *Trans. AIME*, **175**, 184–201 (1948).

Do, D.D., "Dynamics of a Semi-batch Adsorber With Constant Molar Supply Rate: A Method for Studying Adsorption Rate of Pure Gases," *Chem. Eng. Sci.*, **50**, 549–553 (1995).

Do, D.D., "A Model for Surface Diffusion of Ethane and Propane in Activated Carbon," *Chem. Eng. Sci.*, **51**, 4145–4158 (1996).

Do, D.D., "Dynamics of Adsorption in Heterogeneous Solids," in *Equilibria and Dynamics of Gas Adsorption on Heterogeneous Solid Surfaces*, W. Rudzinski, W.A. Steele, and G. Zgrablich (Eds.), p. 777–835, Elsevier, Amsterdam, 1997.

Do, D.D., *Adsorption Analysis: Equilibria and Kinetics*, Imperial College Press, London, 1998.

Do, D.D. and H.D. Do, "A New Adsorption Isotherm for Heterogeneous Adsorbent Based on the Isosteric Heat as a Function of Loading," *Chem. Eng. Sci.*, **52**, 297–310 (1997).

Do, D.D., H.D. Do, and I. Prasetyo, "Constant Molar Flow Semi-batch Adsorber as a Tool to Study Adsorption Kinetics of Pure Gases and Vapours," *Chem. Eng. Sci.*, **55**, 1717–1727 (2000).

Do, D.D. and K. Wang, "A New Model for the Description of Adsorption Kinetics in Heterogeneous Activated Carbon," *Carbon*, **36**, 1539–1554 (1998a).

Do, D.D. and K. Wang, "Dual Diffusion and Finite Mass Exchange Model for Adsorption Kinetics in Activated Carbon," *AIChE J.*, **44**, 68–82 (1998b).

Flood, E.A., R. Tomlinson, and A.E. Leger, "The Flow of Fluids Through Activated Carbon Rods. III. The Flow of Adsorbed Fluids," *Can. J. Chem.*, **30**, 389–410 (1952).

Gilliland, E.R., R.F. Baddour, and J.L. Russell, "Rates of Flow Through Microporous Solids," *AIChE Journal*, **4**, 90–96 (1958).

Higashi, K., H. Ito, and J. Oishi, "Surface Diffusion Phenomena in Gaseous Diffusion. I. Surface Diffusion of Pure Gas," *J. Atomic Energy Society of Japan*, **5**, 846–853 (1963).

Hu, X. and D.D. Do, "Effect of Surface Energetic Heterogeneity on the Kinetics of Adsorption of Gases in Microporous Activated Carbon," *Langmuir*, **9**, 2530–2536 (1993).

Hwang, S.T. and K. Kammermeyer, "Surface Diffusion in Microporous Media," *Can. J. Chem. Eng.*, **44**, 82–89 (1966).

Kainourgiakis, M.E., E.S. Kikkinides, A.K. Stubos, and N.K. Kanellopoulos, "Adsorption Desorption Gas Relative Permeability Through Mesoporous Media—Network Modeling and Percolation Theory," *Chem. Eng. Sci.*, **53**, 2353–2363 (1998).

Kainourgiakis, M.E., A.K. Stubos, N.D. Konstantinou, N.K. Kanellopoulos, and V. Milisic, "A Network Model for the Permeability of Condensable Vapours Through Mesoporous Media," *J. Memb. Sci.*, **114**, 215–225 (1996).

Kaneko, K., N. Setoyama, T. Suzuki, and H. Kuwabana, in *The Fourth Fundamentals of Adsorption*, Kodansha, Tokyo, 1993.

Kapoor, A. and R.T. Yang, "Surface Diffusion on Energetically Heterogeneous Surfaces," *AIChE Journal*, **35**, 1735–1738 (1989).

Kapoor, A. and R.T. Yang, "Surface Diffusion on Energetically Heterogeneous Surfaces—An Effective Medium Approximation Approach," *Chem. Eng. Sci.*, **45**, 3261–3270 (1990).

Kapoor, A., R.T. Yang, and C. Wong, "Surface Diffusion," *Cat. Rev. Sci. Eng.*, **31**, 129–214 (1989).

Karger, J., "Mass Transfer Through Beds of Zeolite Crystallites and the Paradox of the Evaporation Barrier," *Langmuir*, **4**, 1289–1292 (1988).

Kikkinides, E.S., K.P. Tzevelekos, A.K. Stubos, M.E. Kainourgiakis, and N.K. Kanellopoulos, "Application of Effective Medium Approximation for the Determination of the Permeability of Condensable Vapours Through Mesoporous Media," *Chem. Eng. Sci.*, **52**, 2837–2844 (1997).

Lee, C.S. and J.P. O'Connell, "Statistical Mechanics of Partially Mobile Adsorption of Gases on Homogeneous Solid Surfaces," *J. Colloid Interface Science*, **41**, 415–429 (1972).

Lee, C.S. and J.P. O'Connell, "Measurement of Adsorption and Surface Diffusion on Homogeneous Solid Surfaces," *J. Phys. Chem.*, **79**, 885–888 (1975).

Lee, C.S. and J.P. O'Connell, "A Statistical Mechanical Model for Adsorption and Flow of Pure and Mixed Gases in Porous Media With Homogeneous Surfaces. Parts I and II," *AIChE J.*, **32**, 96–114 (1986).

Mayfield, P. and D.D. Do, "Measurement of the Single Component Adsorption Kinetics of Ethane, Butane, and Pentane Onto Activated Carbon Using a Differential Adsorption Bed," *Ind. Eng. Chem. Res.*, **30**, 1262–1270 (1991).

Nicholson, D. and J.H. Petropoulos, "Influence of Adsorption Forces on the Flow of Dilute Gases Through Porous Media," *J. Colloid Interface Science J.*, **45**, 459–466 (1973).

Nicholson, D. and J.H. Petropoulos, "A Fundamental Approach to Molecular Flow in Pore Spaces," *B. der. Bunsen-Gesellshaft*, **79**, 796–798 (1975).

Nicholson, D. and J.H. Petropoulos, "Calculation of the Surface Flow of a Dilute Gas in Model Pores From First Principles. Part II," *J. Colloid Interface Science J.*, **83**, 420–427 (1981a).

Nicholson, D. and J.H. Petropoulos, "Molecular Theory for the Heat of Transport of Dilute Adsorbable Gases in Model Pores," *J. Colloid Interface Science J.*, **83**, 371–376 (1981b).

Nicholson, D. and J.H. Petropoulos, "Calculation of the Surface Flow of a Dilute Gas in Model Pores From First Principles. Part III," *J. Colloid Interface Science J.*, **106**, 538–546 (1985).

Nicholson, D., J. Petrou, and J.H. Petropoulos, "Calculation of the Surface Flow of a Dilute Gas in Model Pores From First Principles. Part I," *J. Colloid Interface Science J.*, **71**, 570–579 (1979).

Petropoulos, J.H., "Model Evaluation of Adsorbate Transport in Mesoporous Media in the Multiplayer Adsorption Region," *Langmuir*, **12**, 4814–4816 (1996).

Popielawski, J. and B. Baranowski, "Statistical Mechanics of Transport Processes in Adsorbed Gases," *Mol. Phys.*, **9**, 59–66 (1965).

Popielawski, J., "The Kinetic Theory of Transport Processes in Adsorbed Gases," *Mol. Phys.*, **10**, 583–594 (1966).

Prasetyo, I., "Kinetics Characterisation of Hydrocarbons on Activated Carbon With new Constant Molar Flow and Differential Permeation Techniques," Ph.D. Thesis, University of Queensland, 2000.

Prasetyo, I. and D.D. Do, "Adsorption Rate of Methane and Carbon Dioxide on Activated Carbon by the Semi-batch Constant Molar Flow Rate Method," *Chem. Eng. Sci.*, **53**, 3459–3467 (1998).

Prasetyo, I. and D.D. Do, "Adsorption Kinetics of Light Paraffins in AC by a Constant Molar Flow Rate Method," *AIChE J.*, **45**, 1892–1900 (1999).

Roybal, L.A. and S.I. Sandler, "Surface Diffusion of Adsorbable Gases Through Porous Media," *AIChE J.*, **18**, 39–42 (1972).

Seidel, A. and P.S. Carl, "The Concentration Dependence of Surface Diffusion for Adsorption on Energetically Heterogeneous Adsorbents," *Chem. Eng. Sci.*, **44**, 189–194 (1989).

Shindo, Y., T. Hakuta, H. Yoshitome, and H. Inoue, "Gas Diffusion in Microporous Media in Knudsen's Regime," *J. Chem. Eng. Jap.*, **16**, 120–126 (1983).

Tamon, H., M. Okazaki, and R. Toei, "Flow Mechanism of Adsorbate Through Porous Media in Presence of Capillary Condensation," *AIChE J.*, **27**, 271–277 (1981).

Wang, K., B. King, and D.D. Do, "Rate and Equilibrium Studies, of Benzene and Toluene Removal by Activated Carbon," *Separation and Purification Technology*, **17**, 53–63 (1999).

Weaver, J.A. and A.B. Metzner, "The Surface Transport of Adsorbed Molecules," *AIChE J.*, **12**, 655–661 (1966).

Yang, R.T., *Gas Separation by Adsorption Processes*, Butterworth, New York, 1987.

Yang, R.T., J.B. Fenn, and G.L. Haller, "Modification to the Higashi Model for Surface Diffusion," *AIChE J.*, **19**, 1052–1053 (1973).